FROM LINEAR TO NON-LINEAR TRANSPORT IN ASYMMETRIC MESOSCOPIC DEVICES*

H. Linke
School of Physics, University of New South Wales
UNSW Sydney 2052, Australia
Physics Department, University of Oregon
Eugene, OR 97403-1274, USA
e-mail: hl@phys.unsw.edu.au

and P. Omling
Solid State Physics, Lund University
Box 118, SE - 221 00 Lund, Sweden
e-mail: Par.Omling@ftf.lth.se

(Received December 6, 2000)

Rocking ratchets are asymmetric potentials operated in the non-linear response regime where rectifying behaviour can be observed. Mesoscopic electronic devices based on semiconductors with low carrier concentration are easily driven away from linear response, and their electron dynamics is at low temperatures altered by quantum effects. Asymmetric semiconductor devices of sub-micron dimensions are therefore suitable for experiments on "quantum ratchets", that is, rocking ratchets based on quantum effects, such as electron interference and tunnelling. We first describe experiments using triangular electron cavities in the linear response regime, illustrating that, at low temperatures, classical and quantum electron dynamics are determined by the shape of the ballistic cavity. Physical reasons for a transition from linear to non-linear behaviour in mesoscopic devices are discussed, and two ratchet experiments in the non-linear regime are described. The sign of rectification in a quantum dot ratchet, based on electron interference effects, depends very sensitively on uncontrollably small deviations from the intended device shape, but can be tuned using parameters such as magnetic field, Fermi energy or the AC voltage. The current direction in a tunneling ratchet can be predicted from the device shape, and is tunable by temperature, when device parameters are suitably chosen.

PACS numbers: 73.23.Ad, 73.50.Fq, 73.40.Ei

* Presented at the XXIV International School of Theoretical Physics "Transport Phenomena from Quantum to Classical Regimes", Ustroń, Poland, September 25–October 1, 2000 and at the XIII Marian Smoluchowski Symposium on Statistical Physics "Fundamentals and Applications", Zakopane, Poland, September 10–17, 2000.

1. Introduction

All materials at finite temperature store a substantial amount of energy in the form of random thermal motion. It is a tempting idea to construct a machine that might put this energy supply to practical use [1,2], but for systems in thermal equilibrium, the Second Law of Thermodynamics safeguards thermal motion from technical exploitation [2]. However, we regularly make use of situations of thermal non-equilibrium to generate useful work, most commonly when using macroscopic heat gradients in heat engines. Recently a more subtle way of extracting work from non-equilibrium has come under detailed investigation (for reviews, see [3-6]). In so-called ratchets, a directed current of particles is generated in the absence of any macroscopic, time-averaged forces or gradients. This is achieved using a combination of spatial or temporal asymmetry, and a source of energy that keeps the system in a state of thermal non-equilibrium. The most well-known example is the "on-off ratchet" illustrated in Fig. 1(a). Here, the combination of, firstly, periodic switching between a flat and a saw-tooth shaped potential, and, secondly, thermal (isotropic) particle diffusion in the off-phase, is converted into directed motion [7,8]. The switching can be random, but needs to happen on a time scale comparable to the time for particle diffusion over one ratchet period. The ratchet can generate a current even against a small external force, using energy that is provided by the switching of the potential, which maintains a situation of thermal non-equilibrium. It is interesting to note, however, that this ratchet mechanism would not work without the random, thermal particle motion in the off-phase. This subtle interplay of thermal motion and a non-equilibrium energy supply is typical for ratchets, and leads to a wide range of interesting phenomena [6]. The principle of the on-off ratchet may also have implications for the force generation on a molecular level in living cells [4,9], and has recently been demonstrated to have potential for particle sorting applications [10].

A second, commonly investigated ratchet type is the "rocking ratchet", consisting of particles in an asymmetric potential which is periodically and symmetrically tilted, or "rocked" (Fig 1(b)). The deformation of an asymmetric potential when tilted depdends on the tilt direction, and in general a net particle current is found when particle motion is averaged over one full cycle of rocking. Unlike the on-off ratchet, a rocked ratchet does not require thermal motion to operate. Particle motion is driven by the tilting force, and it is this external time-dependent field that the ratchet rectifies, not thermal motion. However, as will be shown later (Sect. 5), temperature does have a substantial quantitative and qualitative effect on the ratchet behaviour because it determines the energy distribution of the particles.

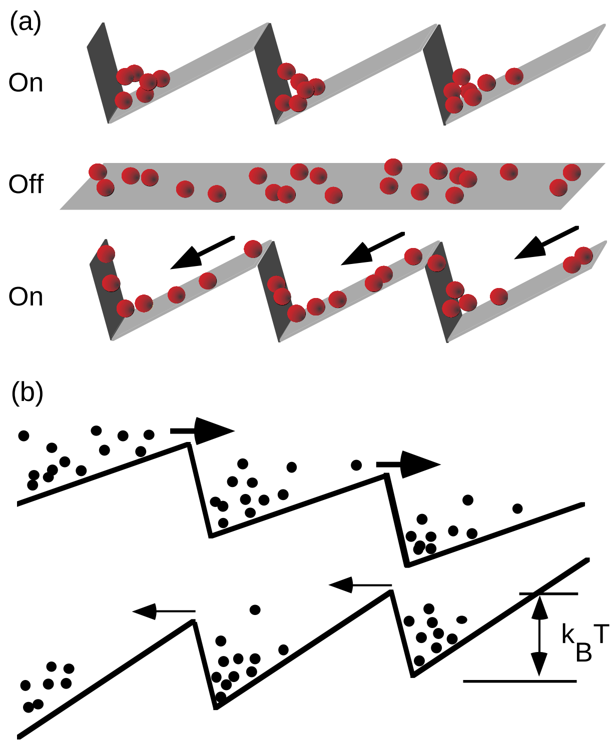

Fig. 1. (a) An on-off ratchet. The periodic, asymmetric potential is switched on and off at a frequency comparable to the time scale for particle diffusion over one potential period. The switching potential serves as a source of non-equilibrium energy, but random particle motion in the off-phase is also required for current generation. (b) A rocking ratchet is essentially a non-linear rectifier. The particle current is different during the two tilt directions, and on time-average a net current is generated.

The physical origin of net current generation in rocking ratchets is the asymmetric, non-linear response of the system to an externally applied force. In the present contribution, we will review recent experiments that make use of the low threshold for non-linear behaviour in small (mesoscopic) electronic devices to observe rectifying effects [11]. At low temperatures, the electronic properties of mesoscopic devices are altered by quantum mechanical effects, such as electron-wave interference or tunnelling. We will show how quantum mechanical behaviour can, in the non-linear response regime, lead to rectification. This enables us to study experimentally the behaviour of "quantum ratchets" [12], that is, rocking ratchets based on quantum effects.

The paper is structured as follows. In Section 2, we introduce our experimental system, electron cavity devices, and a brief review is given of our results on classical and quantum mechanical transport in asymmetric electronic cavities in the linear response regime. In Section 3 we discuss the transition from linear to non-linear transport, which is crucial for the construction of rocking ratchets. Sections 4 and 5 describe two different quantum ratchet effects. First, in Section 4, we describe a "quantum dot ratchet", in which the sensitive response of electron wave interference in electron cavities to an external electric field is used to partially rectify an AC voltage. The behaviour of an asymmetric tunnelling barrier when rocked using a finite AC voltage is described in Section 5. The direction of the generated current is found to depend on temperature, and we present an intuitive explanation for this phenomenon.

2. Triangular electron billiards in the linear response regime

Figure 2 is a scanning electron microscope image of a triangular electron cavity fabricated by electron-beam lithography and shallow wet etching. The darker areas in the image are etched trenches, which serve to interrupt a two-dimensional sheet of electrons (2DEG) located at the interface of a GaAs/AlGaAs heterostructure, typically 30–100 nm below the surface. The trenches electrically isolate the inner part of the triangle, the electron cavity, from the surrounding 2DEG areas, except for two narrow openings (point contacts), visible at the tip and in the centre of the base of the triangle.

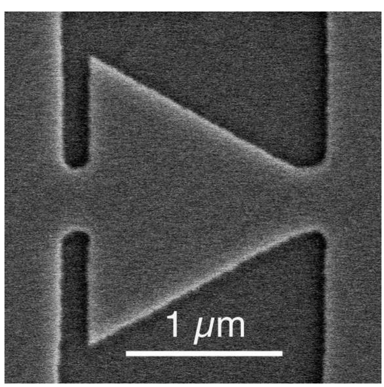

Fig. 2. Scanning electron micrograph of a triangular electron billiard defined by electron beam lithograhy and shallow wet etching. The darker areas have been etched out to electrically interrupt a two-dimensional sheet of electrons located about 70 nm under the surface.

In an experiment, usually a small voltage- or current-bias is applied between the 2DEG areas to the left and right of the device, also referred to as electron reservoirs. The voltage drop over the device is then measured to compute the device conductance. The dimension of electron cavities studied in this way is typically about a micrometer, much smaller than the characteristic length scales for elastic impurity scattering of the host material. By cooling the device to sufficiently low temperatures ($T < 10$ K), also inelastic electron-phonon scattering can be suppressed. In this so-called ballistic limit, the dynamics of electrons inside the cavity are well described by a semi-classical, single-particle picture, in which electrons move on straight directories between boundary collisions [13]. Because of this similarity with a game of billiards, ballistic two-dimensional cavities are often also referred to as electron billiards.

2.1. Classical regime of transport

An experimental perburtation parameter much used to study electron billiards is a perpendicular magnetic field B, which causes the electrons to move on cyclotron orbits with radius $r = m\nu_{\mathrm{F}}/eB$. Here, m and e are the effective mass and the charge of an electron, respectively, and ν_{F} is the velocity at the Fermi energy. In Fig. 3 we show experimental data for the magneto-resistance as well as the result of a computer simulation [14]. The experimental data represented as a dashed line in Fig. 3(a) were taken at temperature of $T = 4.5$ K, sufficiently cold to suppress electron–phonon scattering, but warm enough that effects related to energy quantisation are thermally averaged out. This temperature is thus suitable to study classical transport phenomena in the ballistic regime. The experimental data show strong structure on the normalized field scale B_c, the magnetic field at which the cyclotron diameter equals the side length of the equilateral triangle (for the device used in Fig. 3, $B_c \approx 50$ mT). This is the characteristic magnetic field where one would expect the classical electron dynamics to be notably altered by the field, in agreement with observations [13]. To obtain the simulation shown in Fig. 3(b), electrons that start at Fermi velocity at different initial angles from the opening in the triangle base were traced inside the billiard until they escaped through one of the two contacts. The ratio of the electrons transmitted through the billiard at each setting of the magnetic field, $t(B)$, was determined and then related to the resistance $R(B)$ (no absolute scale) by setting $R(B) \propto 1/t(B)$. The electrons were treated entirely as classical, charged particles in a hard-wall potential, and specular (mirror-like) scattering at the boundaries was assumed. A realistic amount of impurity scattering was taken into account by changing the direction of motion randomly after an exponentially distributed random distance

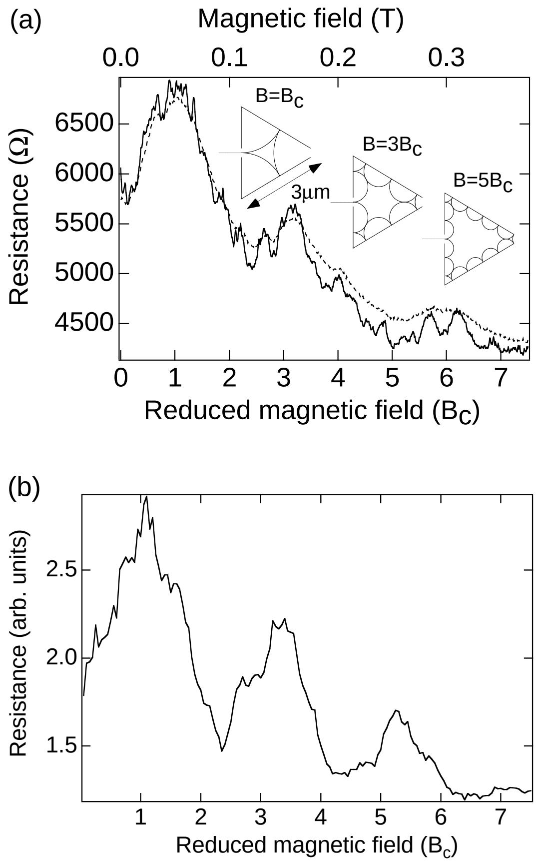

Fig. 3. (a) Magneto-resistance of a triangular billiard at 4.5 K (dashed line), and 0.3 K (full line). Also indicated in (a) are the classical trajectories of electrons that enter the billiard along the symmetry axis through the side opening at $B/B_c =$ 1, 3, 5, respectively, which are thought to be related to the resistance maxima. (b) Classical simulation of the magneto-resistance using a hard-wall potential. Both figures from [15].

of travel (for further details, see [14]). From Fig. 3 it is apparent that the simulation reproduces the overall behaviour of the experimental data taken $T = 4.5$ K, including some fine structures with exception of the statistical noise. In particular, the major resistance maxima at the normalized field B_c, that can be related to the simple, reflected electron trajectories indicated in Fig. 3(a), are reproduced in the simulation. Further analysis allows, in fact, a surprisingly detailed understanding of the magneto-resistance in triangular billiards in terms of specific, classical electron orbits [14–16].

2.2. Quantum regime: conductance fluctuations

The results discussed in the previous section illustrate that electron behaviour in ballistic devices is well described by a single-particle billiard picture, in which electrons are assumed to move undisturbed on classical trajectories. One can take this analysis one step further by considering also quantum mechanical wave interference effects, in addition to the classical dynamics. Experimentally, this is done by lowering the electron temperature below $T \approx 1$ K. Inelastic electron-electron interaction, which is known to suppress electron wave-coherence, a prerequisite for the observation of interference effects, is then suppressed, and the edge of the Fermi distribution is sharp enough to resolve effects related to energy quantisation. In Fig. 3(a) we show as the full line magneto-resistance data taken at $T = 0.3$ K [15]. Superimposed on the classical behaviour discussed above, we observe now rapid fluctuations on a magnetic field scale of a few mT and less, much smaller than the scale $B_c \approx 50$ mT for classical behaviour. While these magneto-conductance fluctuations appear noise-like, they are in fact highly reproducible in subsequent sweeps of B, and are also perfectly symmetric around zero magnetic field.

The origin of magneto-conductance fluctuations (MCF) can be explained in a semi-classical picture, in which a quantum mechanical phase is added to the classical electron trajectories. Typically, the wave length of electrons at the Fermi energy in semiconductor billiards is about 40 nm, or about 20 times smaller than the device, justifying a semi-classical description of transport. Wave interference between pairs of classical electron paths can then be predicted by calculating the electron phase along the classical trajectories. In particular, short, periodic electron orbits can be identified with electron states at energies where a semi-classical Bohr–Sommerfeld quantization condition is fulfilled [17–20]. Transport of electrons through the billiard can then be viewed as a two-step process, in which electrons tunnel through one point contact onto a semi-classical electron state close to the Fermi energy, and then leave this state through the second point contact. The conductance of the billiard is in this picture given by the number of states available at the Fermi energy inside the cavity. A magnetic field shifts the electron phase, and changes the interference. In particular, an electron state related to a specific closed orbit will be switched on and off as the magnetic field is tuned, with a period $\Delta B = h/eA$, given by the ratio of the orbit area, A, and the magnetic flux quantum, (h/e) [21].

Electron-wave interference is extremely sensitive to details of the actual potential inside the billiard, because the typical Fermi wave length is only of order 40 nm. Therefore, and because some imperfections, related to lithography or impurities, are always present, it is not possible to predict MCF in exact detail. MCF are therefore also referred to as a "magnetofingerprint" of a particular device [22]. A statistical analysis based on the macroscopic shape of the device however is possible. In Fig. 3(a), a particular, closed electron orbit is indicated which, as revealed by the classical simulations (Fig. 3 (b)), can be thought of as responsible for the maximum of the classical magnetoresistance apparent at $B = B_c$. In the light of this classical interpretation it is interesting to investigate whether also the quantum fluctuations in the range around $B = B_c$ are related to the orbit shown in Fig. 3(a). To analyse the MCF, we Fourier transform the fluctuations $\Delta G(B) = [G(B, T = 0.3\text{ K}) - G(B, T = 5\text{ K})]$ in the range $0 < B < 1.5B_c$, where $G(B) = 1/R(B)$ stands for the conductance (Fig. 4). Indeed, a peak is found to emerge in the Fourier transformed data, corresponding to a frequency consistent with the area enclosed by the orbit at $B = B_c$ (Fig. 3(a)) [15].

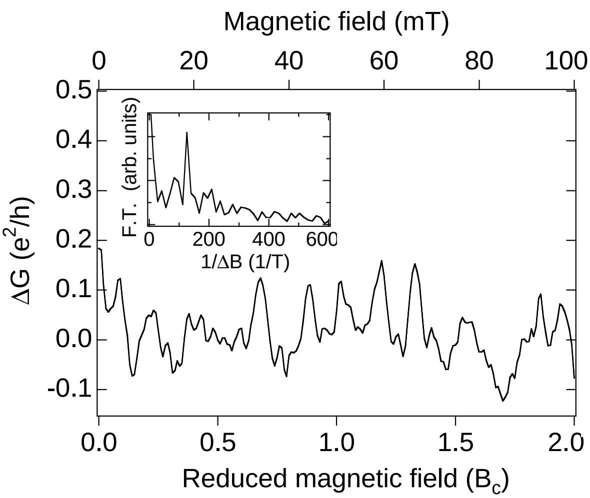

Fig. 4. Conductance fluctuations $\Delta G(B) = [G(B, T = 0.3\text{ K}) - G(B, T = 5\text{ K})]$. In the region of the resistance maximum around $B \approx B_c \approx 50$ mT, the fluctuations are quasi-periodic and the amplitude is enhanced. The inset shows the Fourier transform of the data in the range $0 < B < 1.5B_c$. From [15].

3. From linear to non-linear transport

All experiments described so far have been carried out at very small bias voltage, and non-linear effects were unimportant. In this so-called linear response regime, characterised by a conductance $G = I/V$ which is independent from the voltage V, electron transport is by definition symmetric. No rectification is possible, and a rocking ratchet can not operate. Rectification is represented by the lowest order of non-linearity, that is the term G_1 in the expansion of the current $I(V) = G_0V + G_1V^2 + \ldots$. The term G_1, which can be non-zero only in systems that lack a symmetry axis with respect to the current direction, leads to a finite net current, $I_{\mathrm{net}} = (1/2)[I(V) + I(-V)]$ when a square-wave voltage is applied to the device [11]. Devices where G_1 is finite therefore act as non-linear rectifiers and may be viewed as rocking ratchets.

When does electron transport through a mesoscopic device become non-linear? Electron transport via one-dimensional (1D) wave-modes through a mesoscopic device connecting 2D electron reservoirs can be described by a Landauer equation [23, 24],

$$I(V) = \frac{2e}{h} \int t(\varepsilon, U(V)) M(\varepsilon, V)[f_{\mathrm{S}}(\varepsilon) - f_{\mathrm{D}}(\varepsilon)] d\varepsilon \,. \tag{1}$$

Here, the prefactor $(2e/h)$ is the conductance of each 1D wave-mode, when transmission through the device is perfect. $M(\varepsilon, V)$ is a step function describing the integer number of 1D wave-modes available for transport at each energy, ε. $t(\varepsilon, U(V))$ is the transmission probability for electrons in the respective wave modes and is determined by the device potential, U. f_{S} and f_{D} are Fermi distributions describing the occupation of energy levels in the source- and drain-electron reservoirs, respectively, with electrochemical potentials, μ_{S} and μ_{D}, where $(\mu_{\mathrm{S}} - \mu_{\mathrm{D}}) = eV$.

At very small voltages and temperatures, that is, in the linear response limit, Eq. (1) can be written as $I = 2e^2/hM(\mu_{\mathrm{F}})t(\mu_{\mathrm{F}})V$, where μ_{F} is the equilibrium Fermi energy. To make this approximation, the following conditions need to be fulfilled [24]. Firstly, the transmission probability $t(\varepsilon, U)$ must not vary with energy in the range where electrons contribute to transport. This region is described by the Fermi window, $[f_{\mathrm{S}}(\varepsilon) - f_{\mathrm{D}}(\varepsilon)]$, which has its center within $(\mu_{\mathrm{F}} \pm eV/2)$. A variation of $t(\varepsilon)$ on a scale $\Delta\varepsilon$ does not affect the voltage response, when either $eV \ll k_{\mathrm{B}}T$, or when $(|eV| + 4k_{\mathrm{B}}T) \ll \Delta\varepsilon$. Secondly, for linear response, $t(\varepsilon, U)$ must not depend on the source-drain voltage. The most obvious reason for why $t(\varepsilon, U)$ may be an explicit function of the voltage, is that the device potential itself, U, is distorted by the applied voltage, such that U becomes a function of the voltage, $U = U(V)$. Thirdly, non-linear behaviour is also generated when M is a function of the voltage [25].

Note that, while the variation of t with ε leads to non-linear effects only above a certain threshold given by the energy scale for variation, $\Delta\varepsilon$, and by the temperature, (see above), the variation of t due to a voltage dependence of $U(V)$ has no fundamental threshold. Therefore, non-linear effects can in principle be observed at arbitrarily small voltages. An exact calculation of $t(U(V))$ is in general difficult, and requires the self-consistent solution of the 3D Schrödinger equation including the electric field generated by the voltage across the device, taking into account screening effects. In the following sections, where we will present two different mechanisms leading to asymmetric non-linear behaviour in small devices, we will restrict ourselves to an intuitive description of these phenomena, and will not attempt a detailed discussion of $U(V)$.

4. A quantum dot ratchet

We now return to the triangular electron billiards discussed in Section 2. When studied at low temperatures, where quantum behaviour establishes itself, such devices are often also referred to as "open quantum dots" (for a review, see for instance [26]). To understand the transition from linear to non-linear quantum behaviour it is useful to consider a model for electron transport through quantum dots. Figure 5(a) schematically shows the

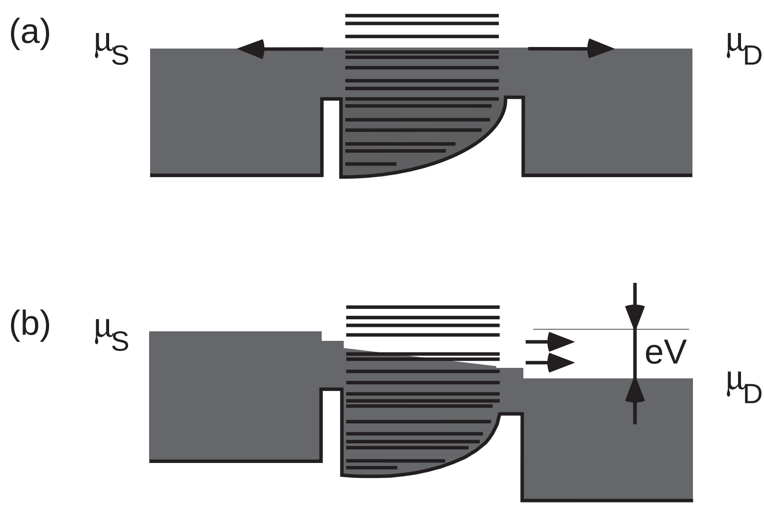

Fig. 5. Illustration of electron transport through a quantum dot. The curvature of the conductance band edge inside the dot represents the effect of the confinement energy inside the triangular dot (not to scale). The horizontal lines inside the dot indicate the shell structure of the density of states. The local electro-chemical potential is indicated by shading. (a) In linear response the transmission probability, that is the conductance, is independent of the absolute value and the sign of the voltage. (b) In the non-linear response regime, the potential and the electron states depend on the applied voltage. Rectification occurs when the potential is not inversion symmetric (see text). From [28].

conduction band bottom along a triangular quantum dot at negligible bias voltage, where the variation of the band bottom represents the effect of the confinement energy in the point contacts and inside the dot. Also shown are the Fermi distribution in the source and drain reservoirs. The effect of energy quantisation inside the dot is represented by horizontal lines indicating a shell structure of the density of states. At very small voltages ($eV \ll \mu_{\rm F}, k_{\rm B}T$), transport through the dot is via the electron states within a few $k_{\rm B}T$ of the Fermi energy [24]. The states that contribute to transport are independent of the applied voltage and are the same for both current directions. This is the linear response regime where transport is by definition symmetric upon voltage reversal. For comparison, Fig. 5(b) shows the situation for finite bias voltage, that is in the non-linear response regime [27,28]. One effect of the bias voltage is to distort the conduction band bottom. How exactly this happens can only be determined in a self-consistent calculation. Here, we are interested in the principle only, and in Fig. 5(b) we assume stepwise voltage drops near the point contacts, and a linear potential slope inside the device. The resulting effective potential landscape $U(V)$, and thus the transmission $t(\varepsilon, U(V))$, depend on the magnitude of the voltage, and, because of the non-symmetric shape of the cavity, also on the voltage sign. This causes non-linear and non-symmetric behaviour of the conductance (Eq. (1)). In addition, at finite bias voltage the width of the Fermi window in Eq. (1) widens, and it's exact position relative to the conductance band bottom inside the dot depends on how the voltage drop is distributed over the device [29]. When the two point contacts are different, as is necessarily the case for a triangular quantum dot, a different range of quantized electron states will contribute for different signs of the voltage [27,28]. Also this effect can be expected to lead to rectification.

Experimental data for the differential conductance $G(V) = \partial I(V)/\partial V$ are shown in Fig. 6. In the experiment, a DC bias voltage was added to a small AC voltage, and the differential resistance was measured as a function of bias voltage using standard phase-locking techniques. The data shown in Fig. 6 were recorded at a series of different magnetic fields, ranging from zero to about ± 18 mT (Figs. 6(a) and (b), respectively), in steps of 2 mT. Three important observations should be made here. Firstly, the conductance clearly depends on bias voltage (non-linear response) in a way that is in general not symmetric with zero bias voltage, that is, rectification is observed. A more detailed analysis shows that most of the asymmetric behaviour is suppressed at temperatures above 1 K, indicating that quantum interference effects are important [27,28]. Secondly, the non-linear effects change rapidly with magnetic field. Importantly, the magnetic field scale (a few mT) is consistent with magnetic-field induced modifications to quantum interference (see Section 2) but not with classical effects (field scale

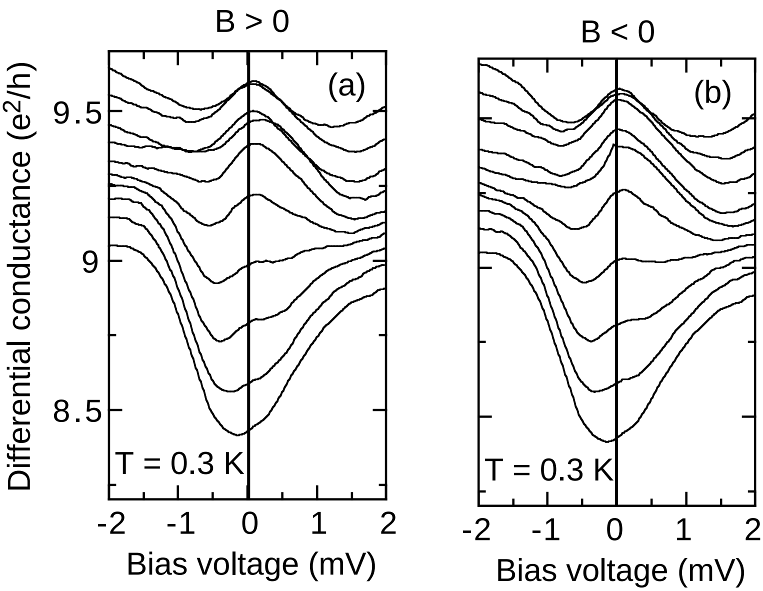

Fig. 6. Experimental data of the differential conductance $G(V)$ at increasing (a) positive and (b) negative magnetic field ($T = 0.3$ K). The field values are from bottom to top for (a) $B = -0.2, +1.8, +3.8,\ \ldots\ ,+17.8$ mT and for (b) $B = -0.2, -2.2, -4.2,\ \ldots,\ -18.2$ mT (note the offset -0.2 mT of the magnetic field values, which is due to a residual field in the magnet). Each curve has been offset by $+0.1e2$/h from the preceding one. From [28].

10–100 mT, see Fig. 3). We can therefore conclude that we observe rectifying behaviour related to the voltage-induced modification of transport through electron quantum states inside the dot, as expected from the discussion above.

A third important observation to be made from Fig. 6 is related to the symmetry in magnetic field. In the linear response regime, conduction is always symmetric with respect to zero magnetic field, that is, the relation $G(B) = G(-B)$ is valid independent of the potential symmetry [24,30]. In the non-linear regime, however, when the conductance depends on the bias voltage, this general symmetry relation breaks down and symmetry in magnetic field is normally absent. The symmetry is restored only when the potential has a symmetry axis parallel to the current direction (Fig. 6). Under this condition, which is fulfilled in our dot geometry, the relation $G(V, B) = G(V, -B)$ should be valid. This symmetry relation allows us to perform an important test: is the origin of rectification in our device indeed the geometry of the dot, and not, for instance, broken symmetry because of random impurities of the material [31–35]? If the answer is “yes”, then the conductance in the non-linear regime should be symmetric with respect to zero magnetic field, because a horizontal symmetry axis should be present. The data shown in Fig. 6 confirm that the non-linear quantum conductance does not depend on the direction of the magnetic field, within a field range that fully alters the non-linear quantum fluctuations. It appears therefore, that any deviations from the intended dot symmetry are not significant within the parameter range covered here ($|B| < 20$ mT, $|V| < 2$ mV), and that the existence of rectification in the asymmetric cavities is indeed related to their asymmetric shape.

The latter observation does not mean, however, that one can predict exactly the direction of rectification of a given device. The reason is, that electron interference is extremely sensitive to small changes of the Fermi energy, of the cavity shape or size, of a small magnetic field (the latter is apparent from Fig. 6), or even of the amplitude of the applied AC voltage [27]. While the sign of rectification is thus not controllable in the fabrication process, it is very easy to adjust the direction of rectification, once it is established, using any of the above parameters.

5. A tunnelling ratchet

We will now describe a different device, one in which tunnelling through an asymmetric barrier is employed to generate a non-linear response to an applied rocking voltage. An SEM image of this tunnelling ratchet is shown in Fig. 7. Crucial for the function of the device as a ratchet is the right hand point contact which forms an asymmetric, 1D wave guide. Electrons travelling along the wave guide need to adjust their lateral wave vector to the channel width. To enter a given part of the channel, electrons therefore require a minimum energy corresponding to the lateral confinement energy. Effectively, the constriction at the point contact thus represents an asymmetric energy barrier (Fig. 8). Using the 2DEG areas above and below the contact as side gates (marked SG), to which a static voltage can be applied, the electrostatic width of the channel, and therefore the height of the effective energy barrier, can be tuned.

The direction of a net current in a rocking ratchet operating classically (Fig. 1(b)) is given simply by the tilt direction in which the effective barrier height is lowest. If the barrier height is independent of the tilt direction, a classical ratchet can not operate. Quantum mechanically, however, particles with an energy below the barrier maximum can tunnel through the classically forbidden barriers, while particles with sufficient energy to cross the barriers may still be wave-mechanically reflected. The corresponding energy-dependent transmission probabilities depend on the exact barrier shape, which will always depend on the tilt direction. With other words,

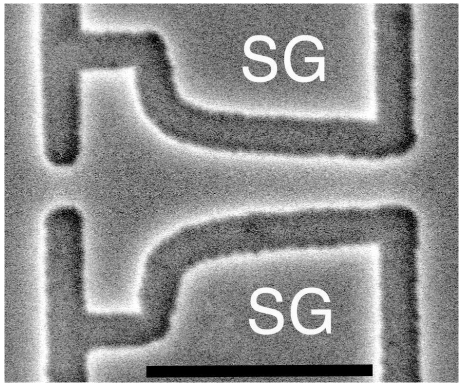

Fig. 7. Scanning electron micrograph of the device used as an electron tunnelling ratchet. Due to confinement energy, the right-hand point contact, which is tunable in width using the side gates SG, forms an asymmetric tunnelling barrier (see Fig. 8). The space bar represents one micrometer.

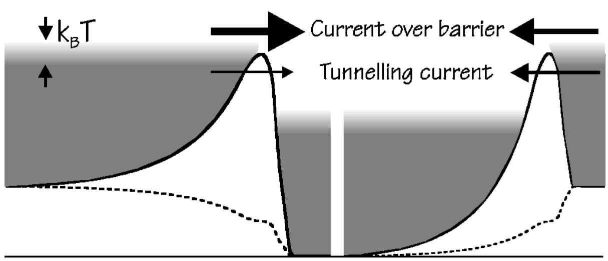

Fig. 8. Schematic drawing of the conducation band bottom of the tunnelling ratchet device shown in Fig. 7, forming an asymmetric energy barrier at the right hand point contact. Both tilt directions are shown. The dashed lines indicate the shape of the assumed voltage drop, which is scaled with the potential gradient of the barrier without tilt (zero bias voltage). For the physical mechanism that leads to a temperature dependence of the total net current direction see text. Figure courtesy of Tammy E. Humphrey.

the transmission probability $t(\varepsilon, U)$ in Eq. (1) is a function of voltage because the potential is a function of voltage, $U = U(V)$. A consequence of this behaviour is that a net current can occur in rocked "quantum ratchets" when this is classically not possible. In addititon, the net current direction can depend on temperature [12], as we will explain in the following.

In Fig. 8 we show an energy barrier, estimated from the dimensions of the device shown in Fig. 7, for both tilt directions, where tilt is generated by applying a positive or negative bias voltage. To predict how the potential deforms under tilt one needs to know the spatial distribution of the voltage drop across the barrier. In Fig. 8, we use a voltage drop distribution that scales with the local gradient of the untilted barrier. The argument behind this assumption is that wave-reflection is stronger when the potential is steeper. In particular, a potential step would be expected to yield a stepwise drop in the conduction band bottom. A side-effect of this particular assumption is that the effective barrier height does not depend on the tilt direction. Therefore, no classical net current is possible, and all net current observed in this model is of quantum mechanical origin. The details of the quantum mechanical current strongly depend on the exact shape of the barrier under tilt, but the following argument holds independent of the exact details of a smooth potential drop across the barrier.

When the barrier is tilted to the right, it deforms to be thicker at a given energy under the barrier top (Fig. 8). This change reduces tunnelling, but, at the same time, makes it easier for electrons with high energy to cross over the barrier, because the smoother shape reduces wave reflection. In the other tilt direction, the barrier deforms to be thinner and sharper, with the opposite effect. Tunnelling becomes easier, but electrons find it more difficult to cross over the top of the barrier, because the steeper potential causes more wave reflection. The result are two contributions to the net current that flow in opposite direction. Averaged over a full period of symmetric rocking, there is a net current to the left consisting of electrons with low energy that tunnel through the barriers. At higher energy, a net current to the right exists, consisting of electrons that pass over the top of the barrier. The direction of the total, energy-averaged net current depends then on the electron energy distribution. At high temperatures, the current to the left will usually dominate, because electrons of higher energy are available. As the temperature decreases, however, this contribution can become smaller than the tunnelling current, and a reversal of the total net current can be observed [12,36].

Experimental data are shown in Fig. 9. A square-wave voltage of amplitude V was applied to the device, and the net current, $I_{\rm net} = (1/2)[I(V) + I(-V)]$, was measured using phase-locking techniques. The frequency used for rocking was of the order of 100 Hz, and was thus much slower than all typical time constants of the electronic system, such as energy relaxation times. The ratchet was therefore at all times in a stationary state. This mode of rocking is called "adiabatic rocking" [12] (note that the word "adiabatic" is elsewhere sometimes used in the opposite sense, that is, for changes that occur fast). Temperature dependence of the current direction due to the mechanism described above is possible when electrons at energies just above and below the barrier top contribute to the current (Fig. 8). To achieve this condition in an experiment, the barrier height is set to approximately match the Fermi energy (the relative position of barrier height and Fermi energy can be estimated from the conductance of the point contact, see Eq. (1)). Further, the rocking voltage, V, is chosen such, that by varying T, the width of the Fermi window, $(|eV| + 4k_{\mathrm{B}}T)$, can be varied over the energy range around the barrier top where quantum corrections to the transmission probability are important. Calculations show that this energy range extends about 1 meV above and below the barrier maximum [36]. In practice, one chooses a suitable rocking voltage and sweeps the barrier height (using the side gates) at various temperatures [36]. In this way one finds sets of values for the rocking voltage and the side gate voltage, where the net current direction depends on temperature. This reversal can then be observed directly by sweeping the temperature while measuring the net current (Fig. 9).

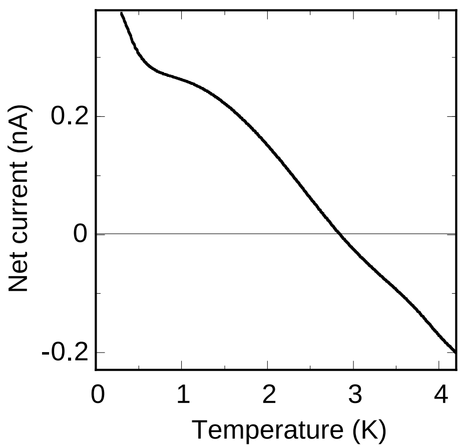

Fig. 9. Measured electrical net current in the tunnelling ratchet device of Fig. 7. Note the reversal of the current direction around $T \approx 2.9$ K. From [36].

In the original work proposing adiabatically rocked quantum ratchets [12], a linear potential drop across the barrier had been considered. The barrier height then depends on the tilt direction, yielding a classical net current. In that work, a reversal with temperature was numerically observed when the thermally excited, classical current decreased with temperature, and the tunnelling contribution counteracted the classical current. In contrast, in the model above (Fig. 8), the classical current is zero, and the current reversal is the result of a competition between tunnelling and quantum mechanical wave-reflection. In general, all three effects, classical effects related to the barrier height, tunnelling, and quantum mechanical wave-reflection, can be important.

6. Conclusion and outlook

We presented a series of experiments demonstrating rectifying behaviour, or ratchet effects, based on non-linear quantum behaviour in asymmetric, mesoscopic electron cavities. Experiments on triangular electron cavities in the linear response regime were described, confirming that the classical as well the quantum mechanical electron dynamics can be described in a semi-classical single-particle picture in which electrons move like billiard balls on classical trajectories between boundary collision. The classical and quantum electron dynamics in ballistic cavities (billiards, or quantum dots) are therfore strongly determined by the shape of the cavity. This behaviour allows to use ballistic cavities to study rectifying effects induced by the shape of the device in the quantum regime. Two specific experiments on rectifying behaviour in the non-linear regime were then described, one based on electron interference (a quantum dot ratchet), and one based on tunnelling through an asymmetric energy barrier (a tunnelling ratchet). The sign of rectification in a quantum dot ratchet depends very sensitively on uncontrollably small deviations from the intended device shape, but can be tuned using parameters such as magnetic field, Fermi energy or the AC voltage. The current direction in a tunneling ratchet can be predicted from the device shape, and is tunable by temperature, when device parameters are suitably chosen.

Both ratchet experiments presented here are examples for so-called adiabatic ratchets, in which potential changes induced by rocking happen on time scales slower than all other relevant time scales of the system. Future work may address the so-called non-adiabatic regime, in which the potential is rocked at a frequency comparable to characteristic times of the particles, such as their escape time through ratchet barriers, or the rate of energy dissipation. In this regime, chaotic behaviour is predicted for moderately damped particles in rocking ratchets [37,38]. Chaos in quantum ratchets may then give rise to novel signatures of quantum chaos in non-equilibrium systems [39]. An experimental realisation of fast potential changes would also allow the construction of so called flashing ratchets, where the potential itself is modified, and no external forces are applied at any time. Flashing ratchets are of interest because these are one candidate for suitable models for some molecular motors in living systems. Regarding quantum effects in ratchets, semiconductor nanostructures are one experimental system in which non-adiabatic quantum ratchets may be realised, others include cold atoms in optical lattices [40].

The authors wish to thank K.F. Berggren, L. Christensson, T.E. Humphrey, P.-E. Lindelof, A. Löfgren, R. Newbury, W.D. Sheng, A.O. Sushkov, A. Svensson, R.P. Taylor, Hongqi Xu and I.V. Zozoulenko for their collaboration.

REFERENCES

[1] M. von Smoluchowski, *Physik. Zeitschr.* **13**, 1069 (1912).

[2] R.P. Feynman, R.B. Leighton, M. Sands, *The Feynman Lectures of Physics*, Vol. Vol. 1, chapter 46, Addison-Wesley, Reading 1963.

[3] P. Hänggi, R. Bartussek, in *Nonlinear Physics of Complex Systems — Current Status and Future Trends*, edited by J. Parisi, S.C. Müller, W. Zimmermann, Springer, Berlin 1996.

[4] R D Astumian, *Science* **276**, 917 (1997).

[5] C. van den Broeck *et al.*, *Lecture Notes in Physics*, Vol. 527, Springer, Heidelberg 1999.

[6] P. Reimann, `cond-mat/0010237`.

[7] J. Rousselet, L. Salome, A. Ajdari, J. Prost, *et al.*, *Nature* **370**, 446 (1994).

[8] For an illustrative simulation applet, see F.J. Elmer, M. Weiß, R. Ketzmerick, `http://monet.physik.unibas.ch/~elmer/bm/` (1998).

[9] F. Jülicher, A. Ajdari, J. Prost, *Rev. Mod. Phys.* **69**, 1269 (1997).

[10] J.S. Bader *et al.*, *Proc. Nat. Acad. Sci.* USA **96**, 13165 (1999).

[11] R. Landauer, in *Nonlinearity in Condensed Matter*, edited by A.R. Bishop, D.K. Campbell, P. Kumar and S.E. Trullinger, Springer Verlag, Berlin 1987.

[12] P. Reimann, M. Grifoni, P. Hänggi, *Phys. Rev. Lett.* **79**, 10 (1997).

[13] For an introduction to ballistic transport in nanostructures, see C.W.J. Beenakker, H. van Houten in *Solid State Physics*, Vol. 44, edited by H. Ehrenreich and D. Turnbull, Academic Press, Boston 1991.

[14] H. Linke, L. Christensson, P. Omling, P.E. Lindelof, *Phys. Rev.* **B56**, 1440 (1997).

[15] L. Christensson, H. Linke, P. Omling, P. E. Lindelof, K.-F. Berggren, I.V. Zozoulenko, *Phys. Rev.* **B57**, 12306 (1998).

[16] P. Bøggild, A. Kristensen, H. Bruus, S.M. Reimann, P.E. Lindelof, *Phys. Rev.* **B57**, 15408 (1998).

[17] M. Persson, J. Pettersson, B. von Sydow, P.E. Lindelof, A. Kristensen, K.F. Berggren, *Phys. Rev.* **B52**, 8921 (1995).

[18] J.P. Bird, D.K. Ferry, R. Akis, Y. Ochiai, K. Ishibashi, Y. Aoyagi, T. Sugano, *Europhys. Lett.* **35**, 529 (1996).

[19] S.M. Reimann, M. Persson, P.E. Lindelof, M. Brack, *Z. Phys.* **B101**, 377 (1996).

[20] For an introduction to semiclassical analysis of electron dynamics in ballistic cavities, see M. Brack, R.K. Badhuri, *Semiclassical Physics*, Addison-Wesley, Reading, MA, 1997.

[21] Y. Aharonov, D. Bohm, *Phys. Rev.* **115**, 485 (1959).

[22] R.P. Taylor *et al.*, *Surf. Sci.* **196**, 52 (1988).

[23] R. Landauer, *Philos. Mag.* **21**, 863 (1970).

[24] For an introduction to one-dimensional transport, see for instance S. Datta, *Electronic Transport in Mesoscopic Systems*, Cambridge University Press, Cambridge 1995.

[25] L.P. Kouwenhoven *et al.*, *Phys. Rev.* **B39**, 8040 (1989).

[26] J.P. Bird, *J. Phys. Condens. Matter* **11**, R413 (1999).

[27] H. Linke, W.D. Sheng, A. Löfgren, H.Q. Xu, P. Omling, P.E. Lindelof, *Europhys. Lett.* **44**, 341 (1998).

[28] H. Linke, Weidong Sheng, A. Svensson, A. Löfgren, L. Christensson, H. Xu, P. Omling, P.E. Lindelof, *Phys. Rev.* **B61**, 15914 (2000).

[29] H. Xu, *Phys. Rev.* **B47**, 15630 (1993).

[30] M. Büttiker, *IBM J. Res. Develop.* **32**, 317 (1988).

[31] R. A. Webb, S. Washburn, C.P. Umbach, *Phys. Rev.* **B37**, 8455 (1988).

[32] S.B. Kaplan, *Surf. Sci.* **196**, 93 (1988).

[33] P.A.M. Holweg *et al.*, *Phys. Rev. Lett.* **67**, 2549 (1991).

[34] D.C. Ralph, K.S. Ralls, R.A. Buhrmann, *Phys. Rev. Lett.* **70**, 986 (1993).

[35] R. Taboryski, A.K. Geim, M. Persson, P.E. Lindelof, *Phys. Rev.* **B49**, 7813 (1994).

[36] H. Linke, T.E. Humphrey, A. Löfgren, A.O. Sushkov, R. Newbury, R.P. Taylor, P. Omling, *Science* **286**, 2314 (1999).

[37] P. Jung, J.G. Kissner, P. Hänggi, *Phys. Rev. Lett.* **76**, 3436 (1996).

[38] J.L. Mateos, *Phys. Rev. Lett.* **84**, 258 (2000).

[39] H. Linke, T.E. Humphrey, R.P. Taylor, A.P. Micolich, R. Newbury, *Phys. Scr.* (2000), in press.

[40] C. Mennerat-Robilliard *et al.*, *Phys. Rev. Lett.* **82**, 851 (1999).